Effect of Angular Acceleration on Brain Injury Metric

Rohit Kelkar, Vikas Hasija and Erik G. Takhounts

Abstract In 1943, Holbourn proposed that brain injury due to rotations is proportional to angular velocity for short duration impacts and is proportional to angular acceleration for long duration impacts. Gabler *et al.* (2016) concluded that angular velocity was sufficient to predict brain injury for impacts of up to 100 ms. The objective of this study was to: (1) evaluate the correlation of a brain injury metric with angular velocity and angular acceleration for short (<100 ms) and long (>100 ms) duration crash events using idealised pulses; and (2) analyse angular velocity and acceleration data from fleet/crash tests and evaluate their feasibility for use in brain injury metric formulation. The study with idealised data demonstrated that both angular velocity and acceleration correlate with brain injury metric up to 100 ms. For crash test data, SAE filtering class CFC 60 resulted in greater peak reduction for angular acceleration (up to 90%), while peak reduction for angular velocity was lower (up to 8%). In addition, collinearity between angular acceleration and velocity was observed when angular accelerations were filtered at CFC 60. Finally, when using crash test data, only angular velocity may be appropriate to use for brain injury formulation.

Keywords Brain injury criteria, Cumulative strain damage measure, Filtering frequency, Rotational brain motion, SIMon FE head model.

I. INTRODUCTION

According to the Centers for Disease Control and Prevention (CDC), traumatic brain injury (TBI) is one of the major causes of death and disability in the USA. TBI can most frequently occur while performing recreational activities and as a result of car accidents or falls [1]. TBI can range from mild to severe, causing a wide range of functional changes affecting thinking, sensation, language and emotion. About 75% of TBI that occur each year are concussions or other forms of mild TBI. In 2014, about 2.87 million TBI-related emergency department visits, hospitalisations and deaths occurred in the USA [2]. Motor vehicle crashes (MVCs) are the third largest cause of TBI-related deaths, accounting for 18.7% of all TBI-related deaths [2] in 2014. The lifetime economic cost of TBI, including direct and indirect medical costs, was approximately $76.5 billion (in 2010 dollars) [3].

In 1943, Holbourn proposed that the rotational motion of the head leads to closed head brain injuries [4]. Concussion and diffuse axonal injury (DAI) are types of closed head injury that result from head rotations [5]. NHTSA has incorporated the Head Injury Criterion (HIC) in regulation for MVCs to account for head injuries in occupants during vehicle impacts [6]. However, HIC does not take rotational motion of the head into consideration. The research on brain injuries due to head rotations has yielded multiple brain injury formulations wherein the rotational kinematic outputs are correlated to brain strains and then used for predicting risk of brain injuries [7]. Cumulative Strain Damage Measure (CSDM) and Maximum Principal Strain (MPS) are two brain strain measurements that are widely used for quantifying brain injury [8-10].

Kleiven [11-12] demonstrated that peak change in angular velocity showed better correlation with the strain levels in the FE head model for purely rotational impulses than angular accelerations or Head Impact Power (HIP). Moreover, Kleiven [13] evaluated the relationship between head kinematics and injury, suggesting that angular velocity components better correlated to mild traumatic brain injury (mTBI) than angular acceleration. Takhounts *et al.* in 2013 proposed a brain injury criterion (BrIC) that considers peak angular velocities in all three directions [8]. BrIC was developed as a correlate to CSDM and MPS. In 2016, Gabler *et al.* suggested that angular velocities are sufficient to predict the brain injury risks for up to 100 ms [10]. A more recent study by Gabler *et al.* [9] proposed that both angular velocity and angular acceleration should be used for head impact durations of 30-40

R. Kelkar (e-mail: rohit.kelkar.ctr@dot.gov; tel: +1-202-366-6208) is a Crash Simulation Engineer and V. Hasija is a Senior Biomechanical Engineer at Bowhead Logistics Solutions. E. G. Takhounts is a Mechanical Engineer at the National Highway Traffic Safety Administration (NHTSA).

ms (typical for MVCs). They developed a brain injury formulation using both peak angular velocities and peak angular accelerations [9] as a correlate to CSDM and MPS. Further, they recommended using the channel frequency class (CFC) 60 filter for angular accelerations [7]. The goals of this study were: (1) to use CSDM and MPS as brain injury measures for determining the effect of various idealised input angular pulses (angular velocity and angular acceleration) on brain injury and determine the correlation between angular pulses and brain injury measures for "realistic" head rotations of up to 90°, assumed to be experienced by occupants in most vehicle crashes; and (2) to analyse angular velocity and angular acceleration data from crash tests and evaluate their feasibility for use in brain injury metric formulation.

II. METHODS

For PART 1 of the study, the SIMon finite element (FE) head model was used, to which idealised angular velocity and angular acceleration pulses were applied. In PART 2, angular velocity and angular acceleration pulses obtained from nine-accelerometer package (NAP) and angular rate sensors (ARS) instrumented crash test dummies (e.g. Hybrid III and THOR 50th percentile male, and ES2) used in various frontal and side impact crash tests (NCAP frontal and side, frontal oblique) were evaluated and analysed.

PART 1

Data

Idealised angular velocity curves were generated using the haversine function, as shown in Equation (1):

$$\omega(t) = \omega * sin^2\left(\pi * \frac{t}{T}\right), \quad (1)$$

where ω = angular velocity amplitude/peak, t = time, and T = impact duration/pulse duration.

A feasibility study was carried out to determine the possible amplitudes/peaks and time durations of the input angular velocity pulses, limited to those that correspond to "realistic" head rotations that may be experienced by occupants in vehicle crashes. A study performed by Ferrario *et al*. [14] showed that the neck range of motion (ROM) was approximately 90° in flexion, 70° in extension, 50° in lateral bending and 90° in axial/transverse plane on both sides. Hence, in this study the "realistic" head rotations for occupants in vehicle crashes were assumed to be limited to 90° (without considering the head rebound that is typically seen at the end of the impact duration in vehicle crashes).

Fig. 1 shows angular velocity plots when the peaks and time durations are increased simultaneously. Corresponding angular acceleration curves obtained by differentiating angular velocity are shown in Fig. 2. When the peak angular velocities were increased simultaneously with the time durations, peak angular accelerations also increased.

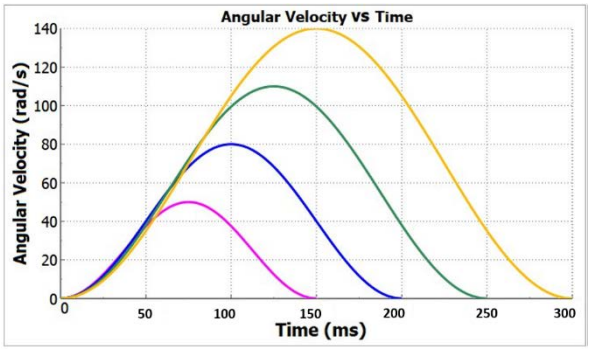

Fig. 1. Angular velocity curves (increasing amplitudes and time duration simultaneously).

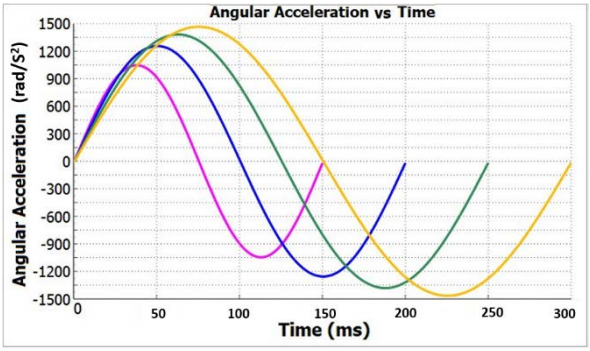

Fig. 2. Angular acceleration curves (differentiated from angular velocity).

However, the maximum head angular displacements obtained by integrating angular velocities (Fig. 1) were unrealistic for humans (between 200° and 1200°, Fig. 3).

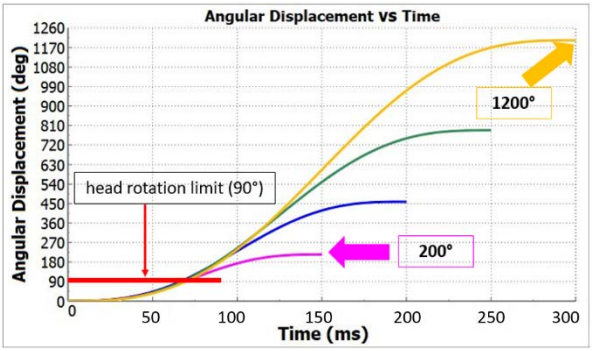

Fig. 3. Angular displacement curves (head rotations).

In order to obtain the realistic head rotations of 90° for occupants of vehicle crashes, the angular velocity amplitudes and time durations cannot increase simultaneously. In this study, to obtain input angular velocity pulses corresponding to realistic head rotations, input angular velocity peaks were varied from 20 rad/s to 100 rad/s with an increment of 10 rad/s (Fig. 4), and corresponding time durations were adjusted such that head kinematics resulted in 90° maximum head rotations (Fig. 5). The corresponding angular accelerations are shown in Fig. 6 and their peaks varied from 390 rad/s^2 (applied over 160 ms) to 10,100 rad/s^2 (applied over 30 ms). The nine resulting pulses include seven that are classified as short duration (<100 ms) and two that are long duration (>100 ms). To capture the possible inertial effects on brain deformation, zero magnitude angular velocity/angular acceleration points were added at the end of the angular velocity/angular acceleration pulses for additional 100 ms (not shown in Figures below for better visualisation).

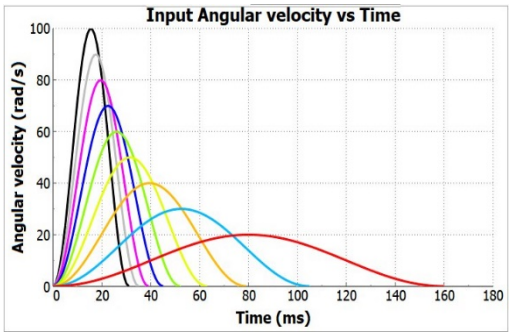

Fig. 4. Input angular velocity curves corresponding to max. head rotations of 90°.

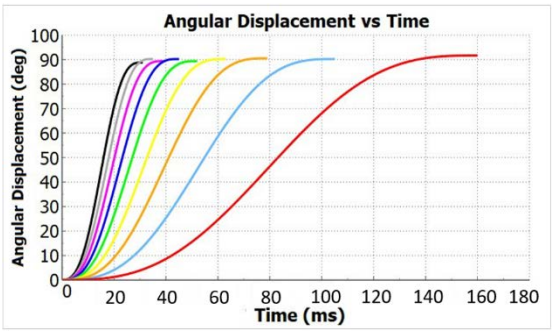

Fig. 5. Angular displacement curves (head rotations).

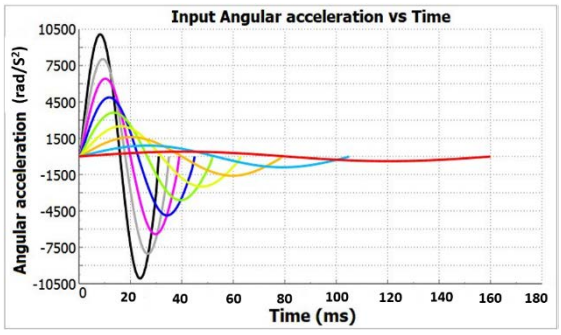

Fig. 6. Input angular acceleration curves (differentiated from angular velocities) corresponding to max. head rotations of 90°.

In this study, the shape of the pulse was not changed whereas the peaks and time durations were changed. This methodology is similar to the one that was used by Kleiven [11-12]. However, this study includes 90° head rotational constraint.

Analysis

A validated SIMon FE head model [15-17] that represents the major parts of the skull and brain, including cerebrospinal fluid (CSF), falx, cerebrum, ventricles, vessels, cerebellum, brain stem and foramen (Fig. 7), was used.

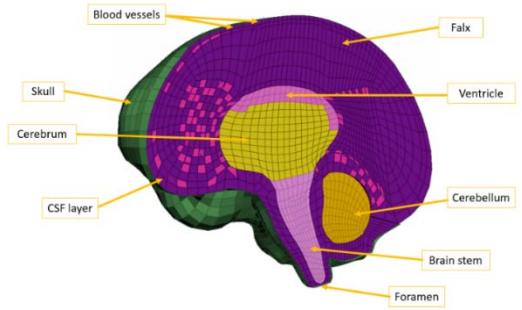

Fig. 7. SIMon Finite Element head model.

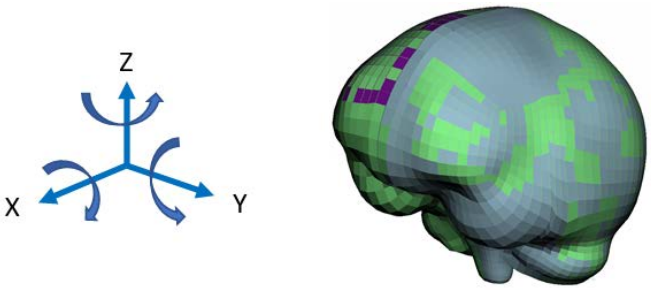

Fig. 8. SIMon FE head model and co-ordinate system for input pulse application.

The pulses shown in Fig. 4 and Fig. 6 were applied to the SIMon FE head model (Fig. 8) about (1) X-axis, (2) Y-axis and (3) Z-axis for a total of 27 simulations. When input pulses were applied about an axis, rotations about the other two axes were constrained (only in-plane rotations were used).

CSDM (0.25) [17] and MPS were computed for all 27 simulations. Effects of long (>100 ms) and short (<100 ms) duration impacts on CSDM and MPS were analysed. Correlations of CSDM (and MPS) with peak angular velocities, peak angular accelerations, and time durations were determined using linear regression. Coefficient of determination (R^2) was used to assess the goodness of fit.

PART2

Data

Angular velocity and acceleration data were obtained from various frontal and side impact crash tests (NCAP frontal and side, frontal oblique) utilising the NAP and ARS instrumentation in Hybrid III, THOR and ES2 anthropomorphic test devices (ATD). One hundred (100) NAP cases and ninety (90) ARS cases were used for performing the analysis. Since the crash test data are noisy as compared to the idealised data from Part 1, these fleet tests based angular velocity and angular acceleration pulses were evaluated for use in brain injury metric formulation by: (a) filtering them at different frequencies and evaluating changes in peaks (this is important because peaks are used in various brain injury metrics); and (b) determining effects of the filtering class on the relationship between peaks of angular accelerations and angular velocities.

Analysis

Butterworth low pass filters with cut-off frequencies of 1650 Hz (CFC 1000) [18], 300 Hz (CFC 180) for ARS data only [18], and 100 Hz (CFC 60) were used for filtering angular pulses. For NAP data, linear accelerations were filtered at CFC 1000 and were used to compute angular accelerations at CFC 1000 [19]. These angular accelerations were then filtered at CFC 60 to obtain angular acceleration at CFC 60. Angular accelerations at CFC 1000 and CFC 60 were integrated to get corresponding angular velocities at CFC 1000 and CFC 60.

For ARS data, angular velocities from ARS were filtered at CFC 1000, CFC 180, and CFC 60. Angular accelerations at CFC 1000 were obtained by differentiating angular velocities at CFC 1000 and angular accelerations at CFC 60 were obtained by differentiating angular velocities at CFC 60 using the central difference method (as per Gabler *et al.*, 2016). A similar procedure was followed to obtain angular accelerations at CFC 180 from angular velocities at CFC 180 as per SAE J211 [18].

For all NAP and ARS cases, the peak values for angular accelerations (filtered at CFC 1000 & CFC 60) and angular velocities (filtered at CFC 1000 & CFC 60) were computed. The percentage difference between the peaks of the same signals, but filtered at CFC 1000 and CFC 60, was then computed.

In addition to peak differences, the following correlations were evaluated: (1) between peak angular acceleration at CFC 1000 and peak angular velocity at CFC 60; (2) between peak angular acceleration at CFC 60 and peak angular velocity at CFC 60. This correlation was carried out for both NAP and ARS data separately and for all data combined. Moreover, for ARS cases, peak values for angular accelerations and angular velocities at CFC 180 were also computed and correlations between 1) peak angular acceleration at CFC 1000 and peak angular velocity at CFC 180 and 2) peak angular acceleration at CFC 180 and peak angular velocity at CFC 180 were analysed [18].

NAP data were further analysed to evaluate the effect of filtering linear accelerations at different frequencies on angular accelerations. First, linear accelerations from NAP data were filtered at CFC 1000 and angular

accelerations were computed at CFC 1000 [19], which were further filtered at CFC 60 to obtain angular accelerations at CFC 60. Second, linear accelerations from NAP were filtered at CFC 60 and then angular accelerations were computed at CFC 60. Angular accelerations obtained from these two methods were compared. The flow chart for this NAP analysis is shown in Appendix A, Fig. A11.

III. RESULTS

PART 1: SIMon FE Model Simulations with Idealised Angular Pulses

Fig. 9 shows input angular velocities (applied about the Y-axis representing pure sagittal plane rotation) and the corresponding CSDM values (line with dots representing a CSDM value corresponding to peak angular velocity and time duration). The colour of each CSDM dot corresponds to the input angular velocity pulse of the same colour. Fig. 9 demonstrates that CSDM values drop with decreased peak angular velocities and increased time durations for the same head rotation of 90°.

For short duration events (<100 ms), CSDM values were significantly higher (between 0.9 and 0.047) as compared to long duration events (>100 ms) (between 0.01 and 0.0048). CSDM becomes negligible (<0.01) for long duration events, indicating that the contribution of peak angular velocity to brain injury is negligible for long duration events. Fig. 10 shows a correlation (R^2 = 0.89) between CSDM and peak angular velocity for short duration events.

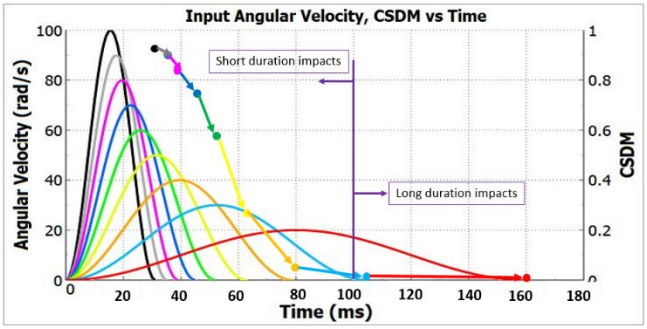

Fig. 9. Angular velocity, CSDM vs Time duration.

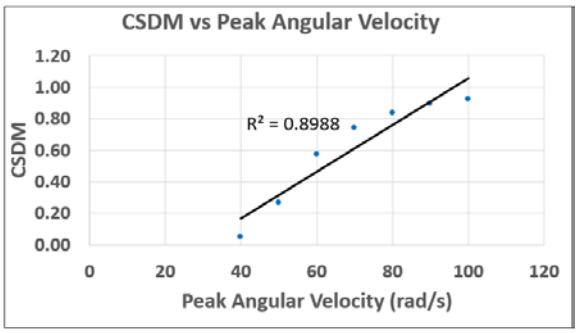

Fig. 10. Correlation plot: CSDM vs Peak angular velocity for short duration events.

Similar observations were made between peak angular acceleration and CSDM values for the nine different time duration angular pulse inputs (Fig. 11). For up to 100 ms, CSDM correlated (R^2 = 0.81) with peak angular accelerations (Fig. 12). Time duration of angular pulses also correlated with CSDM (Fig. 13) for shorter duration impacts with R^2=0.98. The results were similar when angular pulses were applied about X- and Z-axes (Appendix A, Figs A1, A3 & A4).

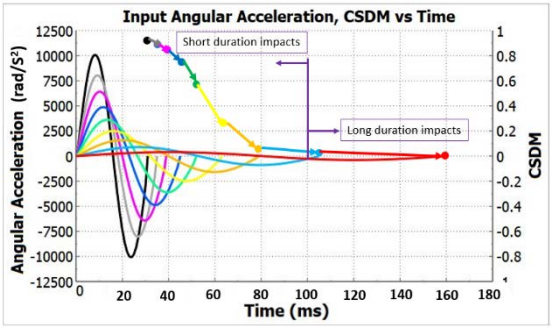

Fig. 11. Angular acceleration, CSDM vs Time duration.

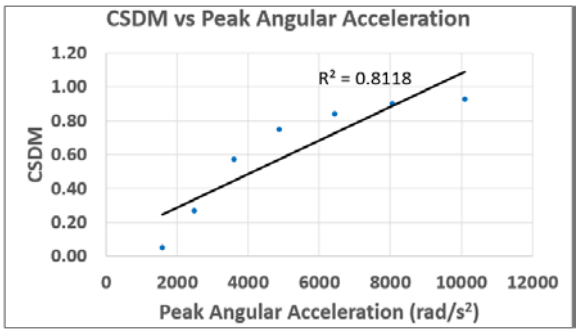

Fig. 82. Correlation plot: CSDM vs Peak angular acceleration for short duration events.

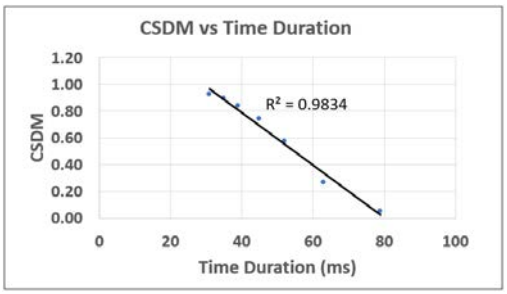

Fig. 13. Correlation plot: CSDM vs Time duration of impact.

Variation of MPS for different angular velocity and angular acceleration pulses are shown in the Fig. A12 and Fig. A13 respectively. The MPS values reduce when peak values decrease and time durations increase for both angular velocity and angular acceleration. MPS also correlated with peak angular velocity (Fig. A5), peak angular acceleration (Fig. A6), and time duration (Fig. A7) for X-, Y-, Z- head rotations until 100 ms. Variation in MPS with time duration for X-, Y-, and Z- head rotations is shown in Fig. A2.

PART 2: Angular pulses from fleet testing and data analysis

Angular data from NAP and ARS collected from fleet testing were compared with idealised data from PART 1. For ARS, comparison of idealised and fleet test based angular velocity is shown in Fig. 14a and Fig. 14b (NHTSA test 9148, frontal oblique offset research test, research vehicle 8200 with 50th percentile adult male THOR ATD) and comparison of idealised and fleet test based angular acceleration is shown in Fig. 15a and Fig. 15b (NHTSA test 9139, frontal oblique offset research test, research vehicle 03EX with 50th percentile adult male THOR ATD).

For the NAP, a comparison of idealised and fleet test based angular velocity is shown in Fig. 16a and Fig. 16b (NHTSA test 4482, vehicle-to-vehicle side impact research test, impacted vehicle – 1999 Chevrolet Prizm with 50th percentile adult male ES2 ATD) and comparison of idealised and fleet test based angular acceleration is shown in Fig. 17a and Fig. 17b (NHTSA test 4205, Frontal NCAP, 2002 Ford Thunderbird roadster with 50th percentile male Hybrid III). It can be observed that the fleet test based angular accelerations are noisy (noisier for ARS than for NAP) as compared to fleet test based angular velocity signals (or idealised angular acceleration signals). Analysis of idealised pulses showed that CSDM (and MPS) is proportional to both peak angular velocities and peak angular accelerations up to 100 ms. To use peak angular acceleration/velocity as a correlate to CSDM and MPS in any brain injury metric formulation, the appropriate filtering class needs to be identified.

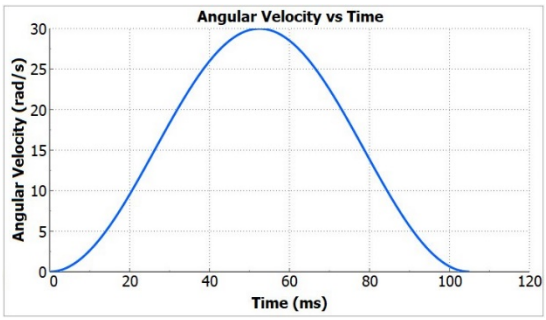

Fig. 14a. Idealised angular velocity.

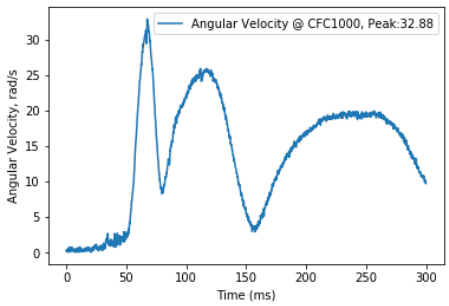

Fig. 14b. Fleet test based ARS angular velocity, filtered at SAE CFC 1000.

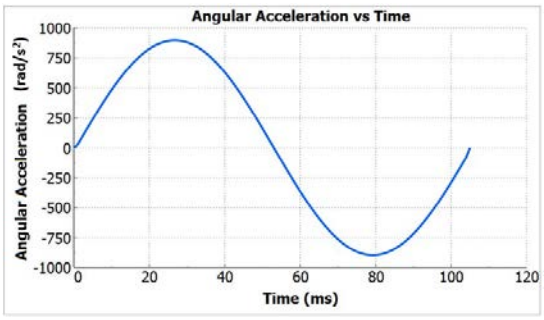

Fig. 15a. Idealised angular acceleration.

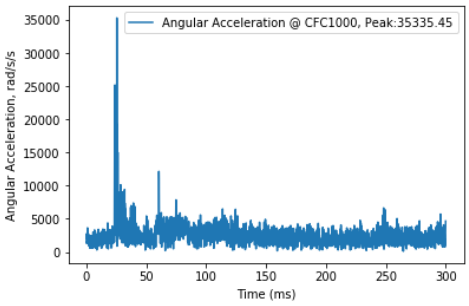

Fig. 15b. Fleet test based ARS angular acceleration, filtered at SAE CFC 1000.

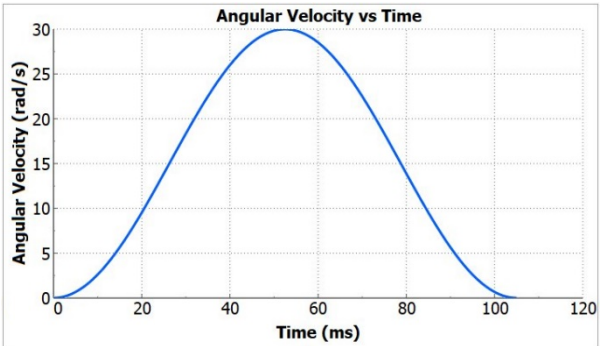

Fig. 16a. Idealised angular velocity.

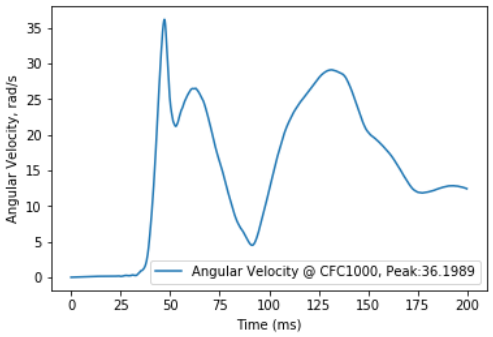

Fig. 16b. Fleet test based NAP angular velocity, filtered at SAE CFC 1000.

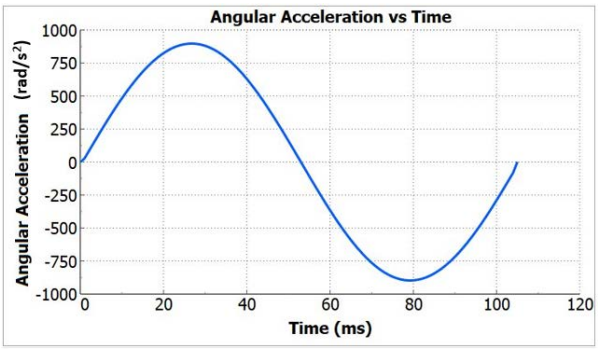

Fig. 17a. Idealised angular acceleration.

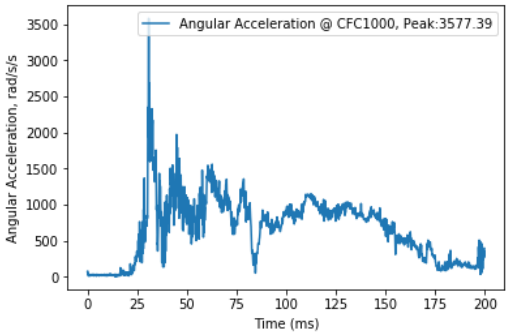

Fig. 17b. Fleet test based NAP angular acceleration, filtered at SAE CFC 1000.

Gabler *et al*. study (2016) recommends using the CFC 60 filter for filtering angular accelerations and angular velocities [7], whereas SAE recommends using CFC 180 filter for angular accelerations and CFC 1000 filter for linear accelerations [18]. To evaluate the feasibility of using the CFC 60 filter, 100 NAP tests and 90 ARS tests were analysed and % peak differences between CFC 60 and CFC 1000 were calculated for each case.

For ARS tests, the % peak difference varied from 0.012% to 4.23% for angular velocity and from 22% to 90% for angular acceleration, whereas for NAP tests % peak difference varied from 0.003% to 8.18% for angular velocity and from 0.78% to 51% for angular acceleration. Fig. 18a and Fig. 18b show the worst cases with respect to % peak difference in angular velocity between CFC 1000 and CFC 60 filtered signals for ARS test (4.23% for NHTSA test 9148) and NAP test (8.18% for NHTSA test 4482), respectively, whereas Fig. 19a and Fig. 19b show the worst cases with respect to the % peak difference for angular acceleration between CFC 1000 and CFC 60 filtered signals for ARS test (90% for NHTSA test 9139) and NAP test (51% for NHTSA test 4205), respectively. Histograms in Fig. 20a and Fig. 20b show the distribution of the % peak difference in angular acceleration across the 90 ARS and 100 NAP cases, respectively. The average % peak difference observed for angular acceleration in ARS was 55% and that in NAP was 13%.

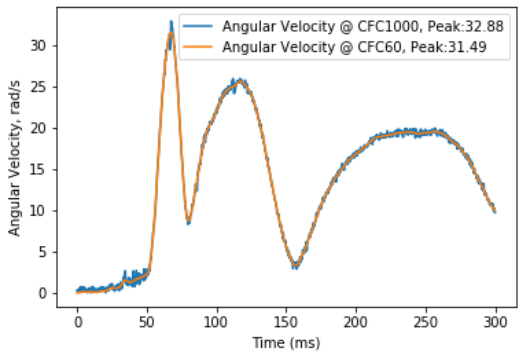

Fig. 18a. Filtered angular velocities (CFC 1000 and CFC 60 - ARS data) for % peak difference calculation.

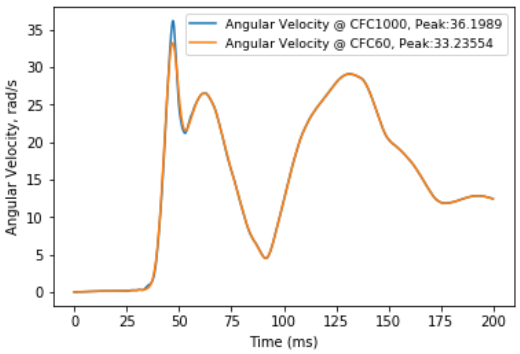

Fig. 18b. Filtered angular velocities (CFC 1000 and CFC 60 - NAP data) for % peak difference calculation.

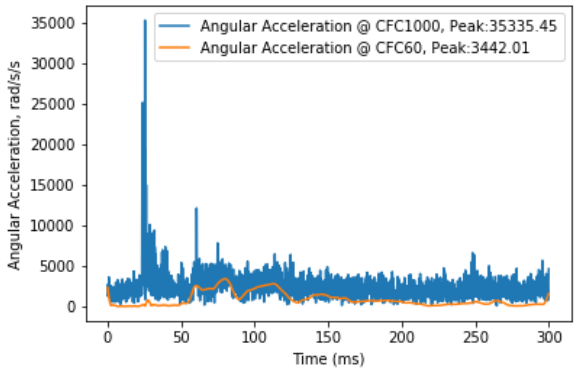

Fig. 19a. Filtered angular accelerations (CFC 1000 and CFC 60 - ARS data) for % peak difference calculation.

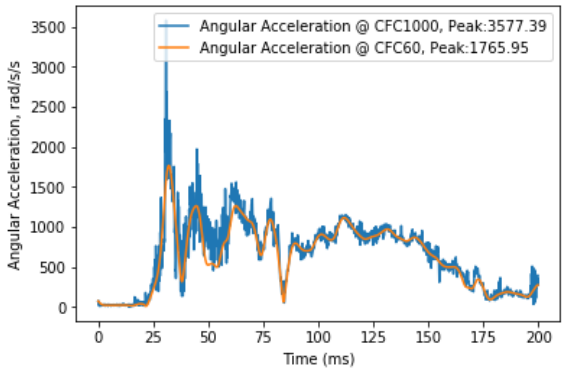

Fig. 19b. Filtered angular accelerations (CFC 1000 and CFC 60 - NAP data) for % peak difference calculation.

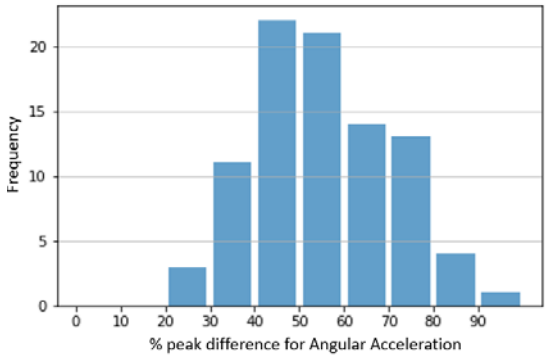

Fig. 20a. Distribution of % peak difference for angular acceleration (ARS data).

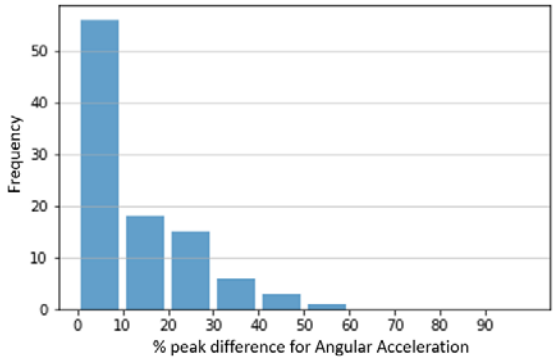

Fig. 20b. Distribution of % peak difference for angular acceleration (NAP data).

To evaluate collinearity, the correlation between angular velocity and angular acceleration was compared at different filtering frequencies. Peak angular accelerations (obtained from CFC 1000 and CFC 60 filtering) were plotted against peak angular velocity (obtained from CFC 60 filtering). This correlation analysis was performed for both NAP and ARS data individually and by combining the two datasets. For ARS data, the correlation was also plotted between peak angular accelerations (obtained from CFC 1000 and CFC 180 filtering) and peak angular velocities (obtained from CFC 180 filtering).

Figures 21a and 21b show correlation between peak angular accelerations (CFC 1000) and peak angular velocities (CFC 60) for ARS and NAP data, respectively. The coefficient of determination (R^2) was 0.03 and 0.27 for ARS and NAP, respectively. The correlation improved from R^2=0.03 to 0.44 for ARS data (Fig. 22a) and from 0.27 to 0.39 for NAP data (Fig. 22b) when peak angular accelerations at CFC 60 were compared with peak angular velocities at CFC 60. For the combined ARS-NAP data, correlation between peak angular acceleration filtered at CFC 1000 and peak angular velocity filtered at CFC 60 was 0.2, and when angular accelerations were filtered at CFC 60 the correlation improved to 0.45 (Appendix A, Fig. A9 and Fig. A10).

For ARS data, the correlation between angular acceleration and angular velocity improved from R^2=0.03 to 0.38 when angular accelerations were filtered at CFC 180 (Appendix A, Fig. A16 and Fig. A17).

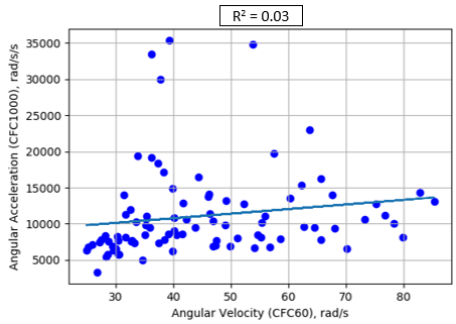

Fig. 21a. Correlation plot between angular acceleration filtered at CFC 1000 and angular velocity filtered at CFC 60 for ARS data.

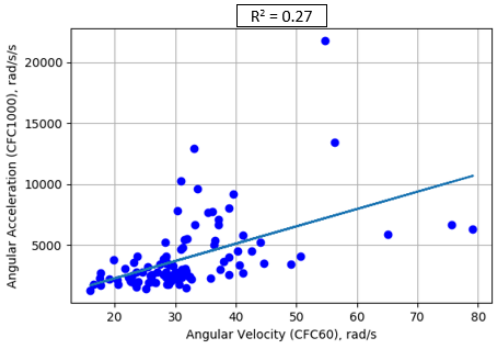

Fig. 21b. Correlation plot between angular acceleration filtered at CFC 1000 and angular velocity filtered at CFC 60 for NAP data.

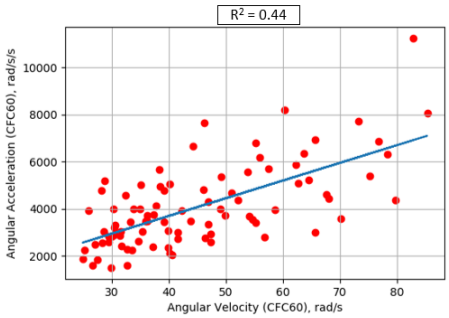

Fig. 22a. Correlation plot between angular acceleration filtered at CFC 60 and angular velocity filtered at CFC 60 for ARS data.

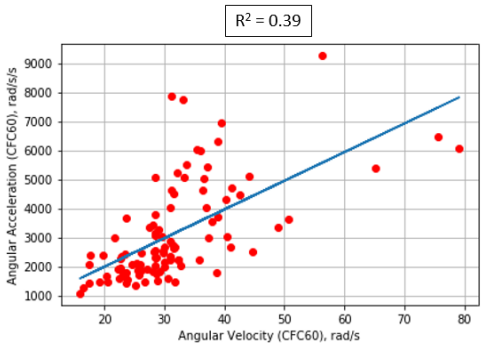

Fig. 22b. Correlation plot between angular acceleration filtered at CFC 60 and angular velocity filtered at CFC 60 for NAP data.

CFC 60 angular accelerations obtained by filtering NAP-based linear accelerations at two different frequencies (Appendix A, Fig. A11) are compared in Fig. 23a and Fig. 23b for two different tests. It is evident from Fig. 23a and Fig. 23b that obtaining angular accelerations at CFC 60 (using CFC 1000 linear accelerations, Method 1, Fig. A11) is identical to filtering linear accelerations at CFC 60 and then computing angular accelerations at CFC 60 (Method 2, Fig. A11).

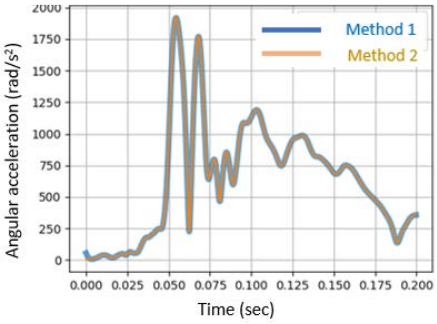

Fig. 23a. Comparison of CFC 60 angular accelerations for NHTSA case 4198.

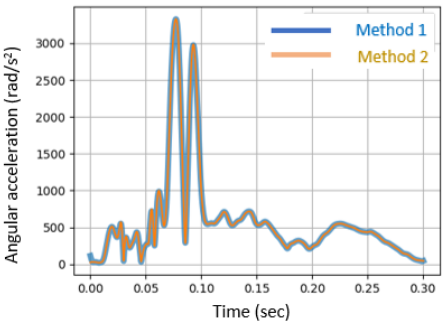

Fig. 23b. Comparison of CFC 60 angular accelerations for NHTSA case 4265.

IV. Discussion

In order to account for brain injuries due to head rotations [4] [20-21], the scientific community has developed various brain injury criteria. It is believed that HIC, which addresses skull/facial fractures, could be used together with the Brain Injury Criterion (BrIC), which addresses rotationally induced brain injuries, to better capture the majority of head injuries [8]. Developed by Takhounts *et al.* [8], BrIC uses peak angular velocities for brain injury risk prediction. In 2018, Gabler *et al.* [9] used peak angular accelerations and velocities, both filtered at CFC 60, to develop a new brain injury criterion (UBrIC) to cover the broader impact conditions.

In this study, the SIMon FE head model was utilised to evaluate the correlation of the brain injury measures, CSDM (Fig. 10, Fig. A3 and Fig. 12, Fig. A4) and MPS (Fig. A5 and Fig. A6), with peak angular velocity and peak angular acceleration using idealised angular pulses with head rotations constrained to those most likely to be

seen in occupants in vehicle crashes. When rotations were constrained to 90° (current study), a strong correlation was observed between CSDM (as well as MPS) and peak angular velocity and angular acceleration in all three directions for short durations (<100 ms). For long duration events (>100 ms), however, peak angular velocity and angular acceleration were significantly smaller and hence no correlation was investigated between angular pulses and CSDM / MPS. MPS values were higher (as opposed to CSDM) for long duration impacts in PART 1 of this study. This is because MPS is reported for each element whereas CSDM considers volume fraction of the brain experiencing a certain strain value. In addition, for long duration pulses, peak angular velocities were lower than 30 rad/s and peak angular accelerations were lower than 900 rad/s^2. For example, angular pulse applied for 160 ms had peak angular acceleration of 390 rad/s^2, with corresponding peak angular velocity of 20 rad/s. According to Ommaya [22], only AIS0 or AIS1 injuries are expected at smaller amplitudes of angular velocity (<30 rad/s) and angular acceleration (<4,500 rad/s^2). In this study, negligible CSDM values (<0.012) were observed in longer duration impacts (>100 ms) for rotations about the X-, Y- and Z-axis, demonstrating that peak angular velocity and peak angular acceleration do not have much effect on brain injury for long duration impacts when head rotations are constrained to those seen by occupants in vehicle crashes. Although peak angular velocities and angular accelerations were not important in long duration crash events, they may become important in other cases of head rotations, such as those experienced by figure skaters, pedestrians, etc. in which the head may move more than 90°. These were not considered in this study.

When idealised pulses were applied to the SIMon FE model, time duration of the crash event also correlated with CSDM (Fig. 13), showing stronger correlation (R^2=0.98) with CSDM compared to peak angular velocity (R^2=0.89) and angular acceleration (R^2=0.81). Despite higher R^2 between time duration and CSDM, it is not feasible for use as an injury metric due to difficulty of identifying the start and end of an event in fleet data, as can be observed in Figs 14b to 17b.

The SIMon FE head model has been validated using neutral density targets (NDT) data where the displacement of the brain relative to the skull was matched for different impacts (frontal, lateral, occipital). Most recently Zhou *et al.* [23-24] evaluated their FE head model against experimental brain strains and this exercise was not carried out for the SIMon FE head model. The limitations of the SIMon FE head model have been described in Takhounts *et al.* [17].

Kleiven [11-12] had performed a study by developing a detailed FE head model and applying angular pulses by changing the durations to determine the effect of different impact directions and durations on the injury. While evaluating the global kinematic injury measure for the rotational pulses, Kleiven found out that change in angular velocity corresponds best with the strains in the FE model. Similar observations were made in this study while comparing correlation between peak angular velocities and CSDM (and MPS) for realistic head rotations of 90°.

PART 1 of this study, using idealised data, demonstrated that CSDM (and MPS) correlates well with both peak angular velocity and peak angular acceleration for short duration events. However, as was shown in PART 2, when fleet test based angular data are considered, the angular pulses are noisy and must be filtered prior to utilisation of their peaks in development of brain injury metrics. Gabler *et al.* [7] study recommends using CFC 60 for filtering both angular velocities and angular accelerations. When different filters (CFC 1000 and CFC 60) were used in the current study, differences between the peaks of angular accelerations were significantly higher than those of angular velocities. Hence, in choosing a kinematic metric as a correlate for CSDM (or MPS) when using crash test data, it is important to consider one for which the magnitude is less dependent on the filtering frequency. In this case, it is angular velocity. In addition to significant peak losses for angular accelerations, computing angular accelerations using different methods leads to different time histories. When the methodology described in Gabler *et al.* [7] was used for obtaining the angular accelerations at CFC 60 using angular velocities at CFC 60 (central difference method), it was observed, when comparing angular acceleration at CFC 1000 and at CFC 60 (Fig. A14) that for some cases peaks occurred at different times. In addition, peak values of angular accelerations (CFC 60) for these cases obtained by Gabler *et al.* method were different than peak values of angular accelerations (CFC 60) obtained from angular accelerations at CFC 1000, e.g. Fig. A14 has a peak value of 3600 rad/s^2 whereas Fig. A15 shows a peak value of 10,000 rad/s^2 for angular acceleration at CFC 60. When angular accelerations at CFC 1000 were filtered to obtain angular accelerations at CFC 60, the peaks were at the same time for all cases (e.g. Fig. A15). Additionally, Takhounts *et al.* [8] had used the fleet /crash test pulses that are utilized in current study and they demonstrated that peak angular accelerations do not correlate well with CSDM (or MPS).

One of the important assumptions of linear regression is that there should be little or no multicollinearity (or

collinearity) between independent parameters that are used for predicting a dependent variable (brain injury measures in our case) [25-26]. Collinearity is a condition in which some of the independent parameters (predictor variables) are highly correlated. In PART 2 of this study, filtering angular accelerations at CFC 60 led to artificial collinearity (increased R^2) between peak angular velocities and peak angular accelerations. This collinearity could result in misleading interpretation of the results [25]. Collinear variables when used in constructing various models tend to overfit, and overfitted models fail to replicate in future samples [26]. Thus, using both peak angular accelerations and peak angular velocities filtered at CFC 60 as predictor variables for brain injury metrics may not be appropriate due to artificially created (by such filtering) collinearity between the two variables.

In addition to artificially created collinearity, if angular acceleration is used in the brain injury metric formulation, it either needs to be computed from NAP (from linear accelerations at CFC 1000) or from ARS. In Gabler *et al.* (2016) angular velocities were filtered at CFC 60 to obtain angular accelerations, whereas, SAE J211 [18] recommends using CFC 180 for filtering angular velocities to obtain angular accelerations. If low pass frequency filter (such as CFC 60) is used for filtering angular accelerations, it "washes away" the differentiating power of measurement between angular acceleration and velocity (R^2 increases from 0.03 to 0.44 for ARS and from 0.27 to 0.39 for NAP, Fig. 21-22). The use of higher CFC filter class (such as CFC 1000) would preserve the differentiating power, which may be feasible for angular accelerations. However, in that case there is no correlation between angular acceleration and brain injury measurement [8]. On the other hand, the angular velocity is hardly affected by the filtering frequency for both NAP and ARS data. Also, angular velocity is much less susceptible to metal-on-metal induced noise and other factors that could perturb the signal during a crash test.

Finally, the NAP data analysis (Fig. 23a and Fig. 23b) in this study demonstrated that filtering angular accelerations at CFC 60 is similar to filtering linear accelerations at CFC 60. SAE J211 recommends filtering linear accelerations at CFC 1000 [18]. Thus, filtering angular accelerations at CFC 60 may not be appropriate.

V. CONCLUSIONS

The following are the conclusions of this study.

- For idealised pulses, when head rotations are constrained to realistic head rotations (90°) for occupants in vehicle crashes, brain injury measures (CSDM and MPS) correlated with peak angular velocity and peak angular acceleration for short duration impacts (<100 ms).
- CSDM becomes negligible for long duration impacts (>100 ms), indicating that neither peak angular velocity nor peak angular acceleration has an effect on CSDM, when head rotations are constrained to 90°.
- When considering fleet test data, peak angular accelerations are highly dependent on the filtering frequency and the instrumentation package used, and the difference between peaks of angular accelerations filtered at CFC 1000 and CFC 60 are significantly higher than those between peaks of angular velocities.
- Converting angular velocities (CFC 60) to angular accelerations (CFC 60) as per the procedure followed in Gabler *et al.* [7], in some cases, causes the peaks of angular accelerations at CFC 1000 and at CFC 60 to occur at different times.
- In some cases, the peak values of angular accelerations (CFC 60) and time at which they occurred are different, when angular accelerations (CFC 60) are obtained from angular velocity (CFC 60, Gabler *et al.* methodology) and from angular acceleration (CFC 1000).
- Artificial collinearity is created between peak angular accelerations and peak angular velocities when angular accelerations are filtered at CFC 60.
- Application of SAE CFC 60 filter to fleet test based angular accelerations may not be appropriate.
- Peak angular velocity is a more appropriate kinematic parameter in the search for a better correlate to CSDM because of smaller variability (as opposed to peak angular acceleration) when using any filtering class for any instrumentation (ARS or NAP).

VI. REFERENCES

[1] Talebanpour, A., Smith, L., (2017) A Comparison Between Simulated and Measured Human Brain Response under Mild Acceleration. *Proceedings of IRCOBI Conference*, 2017, Belgium.

[2] Centers for Disease Control and Prevention (2019) Traumatic Brain Injury & Concussion. Internet: https://www.cdc.gov/traumaticbraininjury/data/index.html, 29, March 2019 [Accessed 6 January 2020].

[3] Centers for Disease Control and Prevention (2019) Traumatic Brain Injury & Concussion. Internet: https://www.cdc.gov/traumaticbraininjury/severe.html, April 2019 [Accessed 6 January 2020].
[4] Holbourn, A. H. S. (1943) Mechanics of head injury. *The Lancet* (9 October): pp.438–441.
[5] Gennarelli, T. A., Lawrence, E., *et al*. (1982) Diffuse Axonal Injury and Traumatic Coma in the Primate. *Annals of Neurology*, **12**(6).
[6] Eppinger, R., Sun, E., *et al.* (1999) Development of Improved Injury Criteria for the Assessment of Advanced Automotive Restraint Systems – II. NHTSA, Washington DC, USA, November 1999, pp.2-1–2-11.
[7] Gabler, L. F., Crandall, J. R., Panzer, M. B. (2016) Assessment of Kinematic Brain Injury Metrics for Predicting Strain Responses in Diverse Automotive Impact Conditions. *Annals of Biomedical Engineering*, **44**(12): pp.3705–3718, Epub – 19 July 2016.
[8] Takhounts, E. G., Craig, M. J., Moorhouse, K., McFadden, J., Hasija, V. (2013) Development of Brain Injury Criteria (BrIC). *Stapp Car Crash Journal*, **57**: pp.243–266.
[9] Gabler, L. F., Crandall, J. R., Panzer, M. B. (2018) Development of a Metric for Predicting Brain Strain Responses Using Head kinematics. Annals of Biomedical Engineering, **46**(7): pp.972–985, Epub - 28 March 2018.
[10] Gabler, L. F., Crandall, J. R., Panzer, M. B. (2016) Investigating Brain Injury Tolerance in the Sagittal Plane Using a Finite Element Model of the Human Head. *International Journal of Automotive Engineering*, **7**: pp.37–43.
[11] Kleiven, S. (2005) Influence of Direction and Duration of Impacts to the Human Head Evaluated Using the Finite Element Method. *Proceedings of IRCOBI Conference*, 2005, Czech Republic.
[12] Kleiven, S. (2006) Evaluation of Head Injury Criteria Using a Finite Element Model Validated Against Experiments on Localized Brain Motion, Intracerebral Acceleration, and Intracranial Pressure. IJCrash, **11**(1): pp.65–79.
[13] Kleiven, S. (2007) Predictors for Traumatic Brain Injuries Evaluated through Accident Reconstructions. *Stapp Car Crash Journal*, **51**: pp.81–114.
[14] Ferrario, V. F., Sforza, C., Serrao, G., Grassi, G., Mossi, E. (2002) Active range of motion of the head and cervical spine: a three-dimensional investigation in healthy young adults. Journal of Orthopedic Research, **20**: pp.122–129, May 2001.
[15] Bandak, F. A., Zhang, A. X., *et al.* (2001) SIMon: A SIMULATED INJURY MONITOR; APPLICATION TO HEAD INJURY ASSESSMENT. *International Technical Conference on Enhanced Safety of Vehicles*, June 2001, Netherlands.
[16] Takhounts, E. G., Eppinger, R. H., *et al*. (2003) On the Development of the SIMon Finite Element Head Model. *Stapp Car Crash Journal*, **47**: pp.107–133.
[17] Takhounts, E. G., *et al.* (2008) Investigation of Traumatic Brain Injuries Using the Next Generation of Simulated Injury Monitor (SIMon) Finite Element Head Model. *Stapp Car Crash Journal*, **52**: pp.1–32.
[18] SAE J211-1 (2014) Instrumentation for Impact Test - Part1 - Electronics Instrumentation, page 8, SAE International, Warrendale, PA, USA, March 2014.
[19] Padgaonkar, A. J., Krieger, K. W., King, A. I. (1975) Measurement of Angular Acceleration of a Rigid Body Using Linear Accelerometers. Journal of Applied Mechanics, **42**(3): pp.552–556.
[20] Gennarelli, T. A., Thibault, L. E., Ommaya, A. K. (1972) Pathophysiologic Responses to Rotational and Translational Accelerations of the Head. *Stapp Car Crash Journal*, **16**: pp.296–308.
[21] Ueno, K., Melvin, J. W. (1995) Finite element model study of head impact based on hybrid III head acceleration: The effects of rotational and translational acceleration. *Journal of Biomechanical Engineering*, **117**(3): pp.319–328.
[22] Ommaya, A. K. (1985) Biomechanics of Head Injury: Experimental Aspects. *The Biomechanics of Trauma, Nahum*, A. M. and Melvin, J. W. (eds), Appleton-Century-Crofts, Holland pp.245–269.
[23] Zhou, Z., Li, X., Kleiven, S., Hardy, W. N. (2019) Brain Strain from Motion of Sparse Markers. *Stapp Car Crash Journal*, **63**: pp.1–27.
[24] Zhou, Z., Li, X., Kleiven, S., Shah, C. S., Hardy, W. N. (2018) A Reanalysis of Experimental Brain Strain Data: Implication for Finite Element Head Model Validation. *Stapp Car Crash Journal*, **62**: pp.293–318.
[25] Vatcheva, K. P., Lee, M., McCormick, J. B., Rahbar, M. H. (2016) Multicollinearity in regression analyses Conducted in Epidemiologic Studies. *Epidemiology* (Sunnyvale). 2016 April 6(2) doi:10.4172/2161-1165.1000227, Epub 2016 Mar 7.
[26] Babyak, M. A. (2004) What You See May Not Be What You Get: A Brief, Nontechnical Introduction to Overfitting in Regression-Type Models. *Psychosomatic Medicine*, **66**(3): pp.411–421.

VII. APPENDIX A

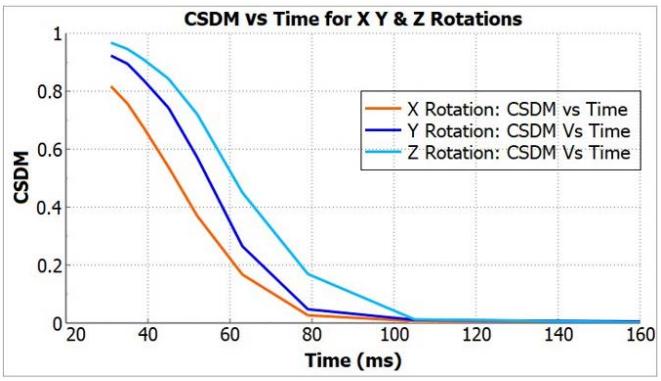

Fig. A1. Comparison of CSDM vs Time (impact duration) plot for head rotations about X, Y and Z.

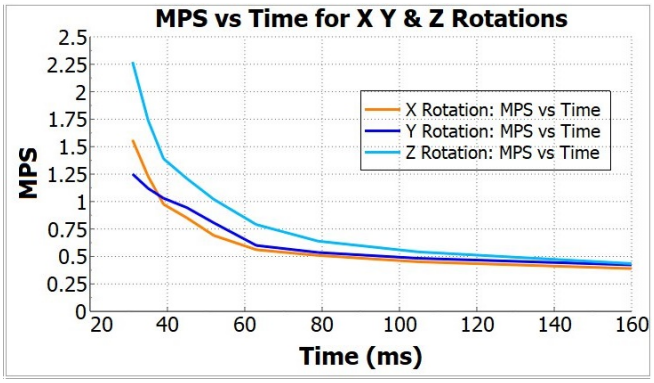

Fig. A2. Comparison of MPS vs Time (impact duration) plot for head rotations about X, Y and Z.

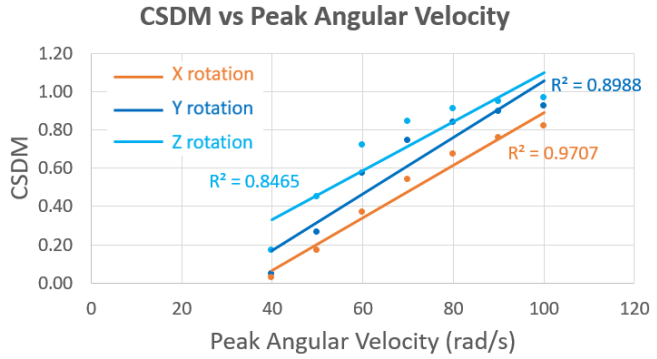

Fig. A3. Correlation plot: CSDM vs Peak angular velocity (X, Y, Z rotations).

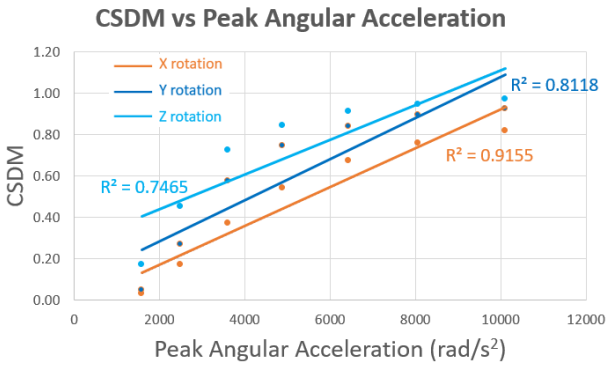

Fig. A4. Correlation plot: CSDM vs Peak angular acceleration (X, Y, Z rotations).

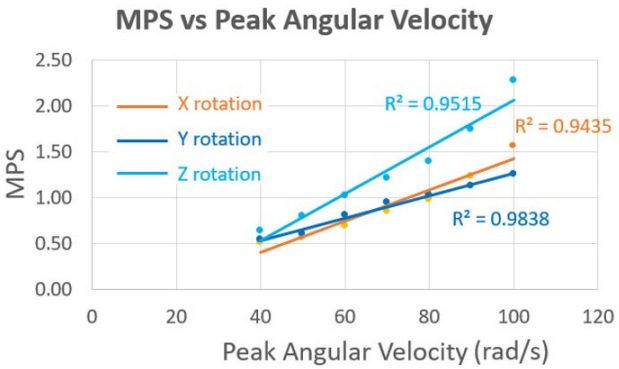

Fig. A5. Correlation plot: MPS vs Peak angular velocity (X, Y, Z rotations).

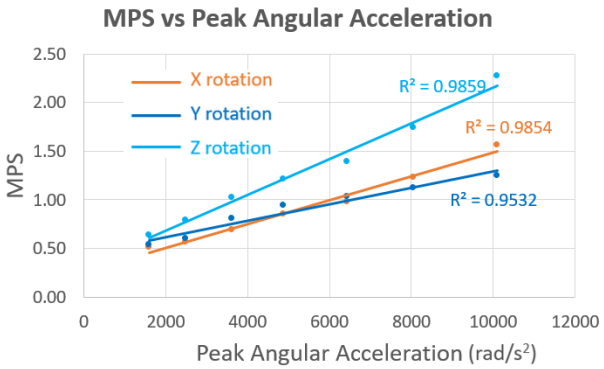

Fig. A6. Correlation plot: MPS vs Peak angular acceleration (X, Y, Z rotations).

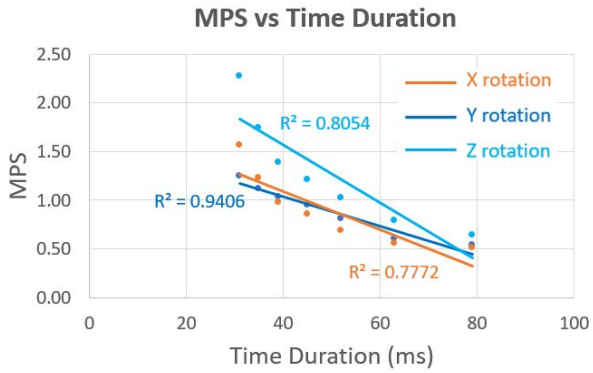

Fig. A7. Correlation plot: MPS vs Time duration of impact (X, Y, Z rotations).

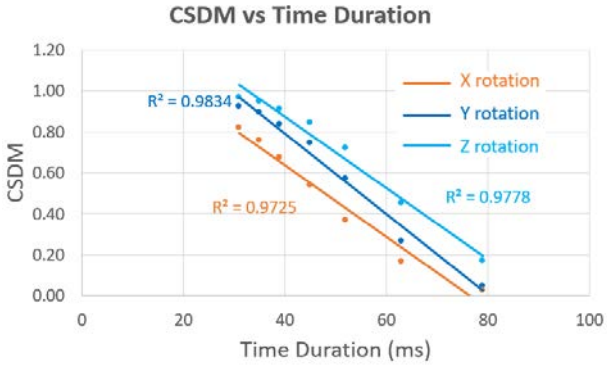

Fig. A8. Correlation plot: CSDM vs Time duration of impact (X, Y, Z rotations).

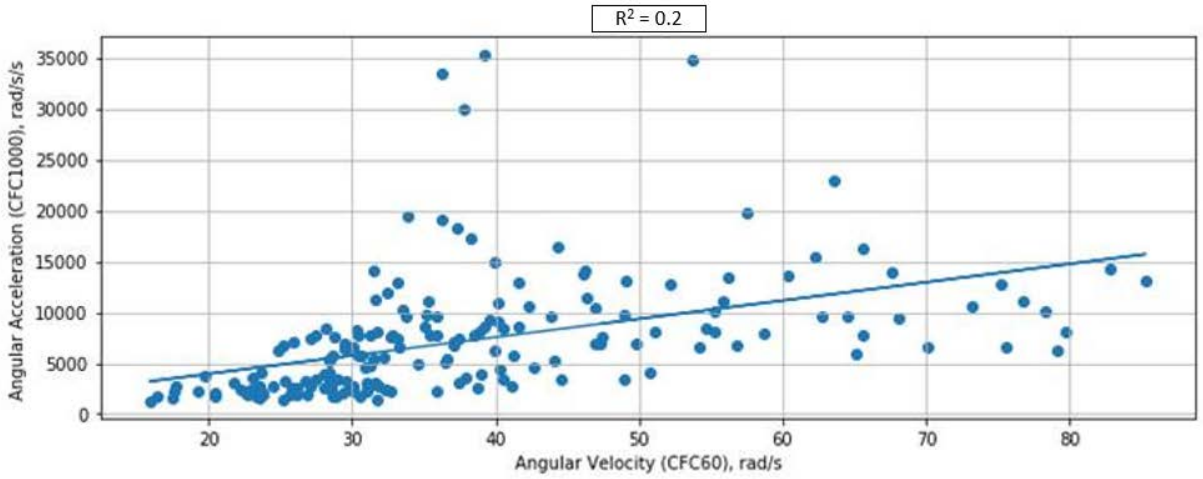

Fig. A9. Correlation between peak angular accelerations (CFC 1000) and peak angular velocities (CFC 60) for combined ARS and NAP data.

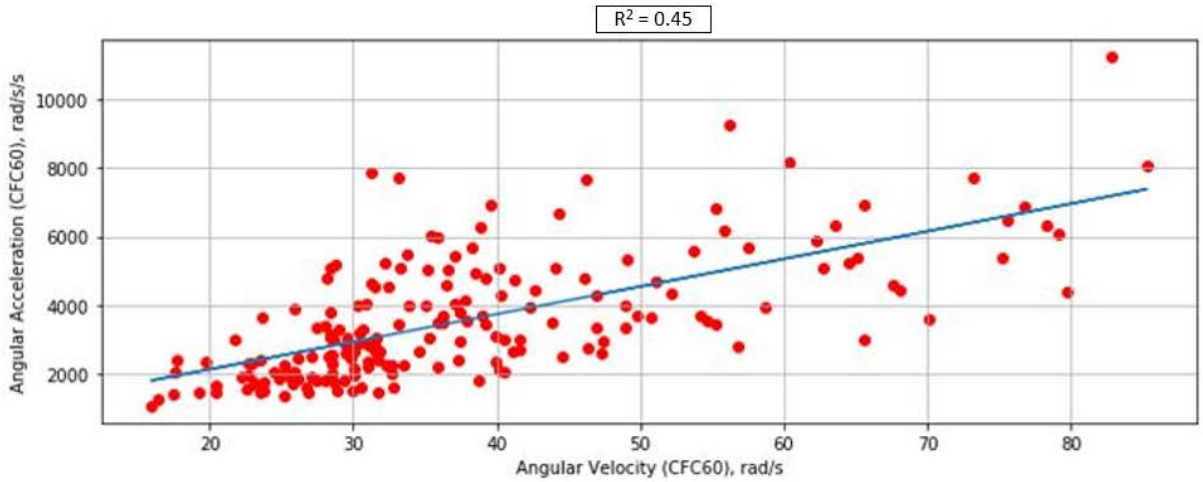

Fig. A10. Correlation between peak angular accelerations (CFC 60) and peak angular velocities (CFC 60) for combined ARS and NAP data.

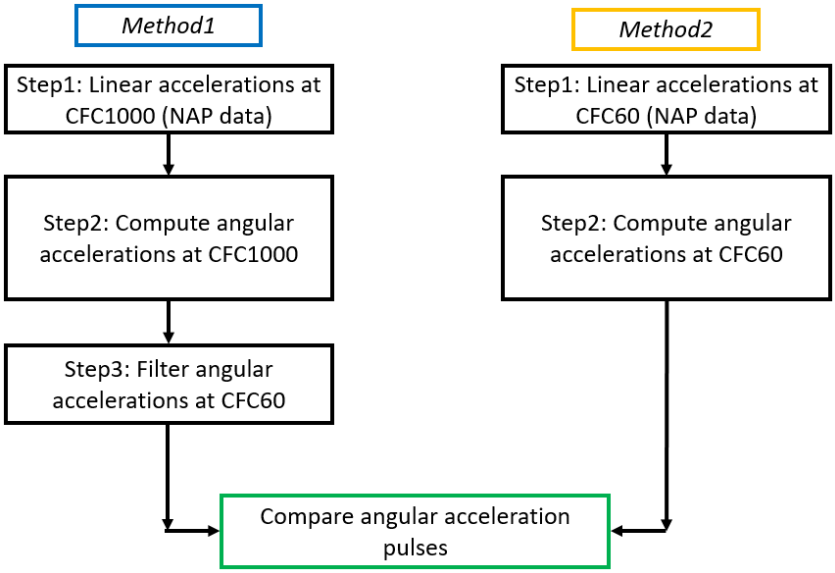

Fig. A11. Flow chart with two different methods for calculating angular acceleration pulses at CFC 60 from linear acceleration pulses (NAP data). Method 1: filtering linear accelerations at CFC 1000. Method 2: filtering linear accelerations at CFC 60.

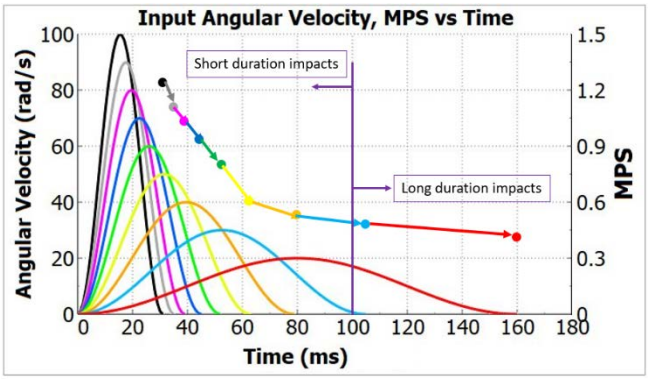

Fig. A12. Angular velocity, MPS vs Time duration (Y-rotation).

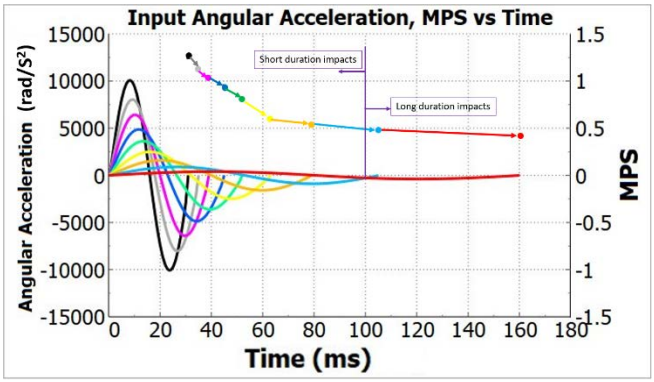

Fig. A13. Angular acceleration, MPS vs Time duration (Y-rotation).

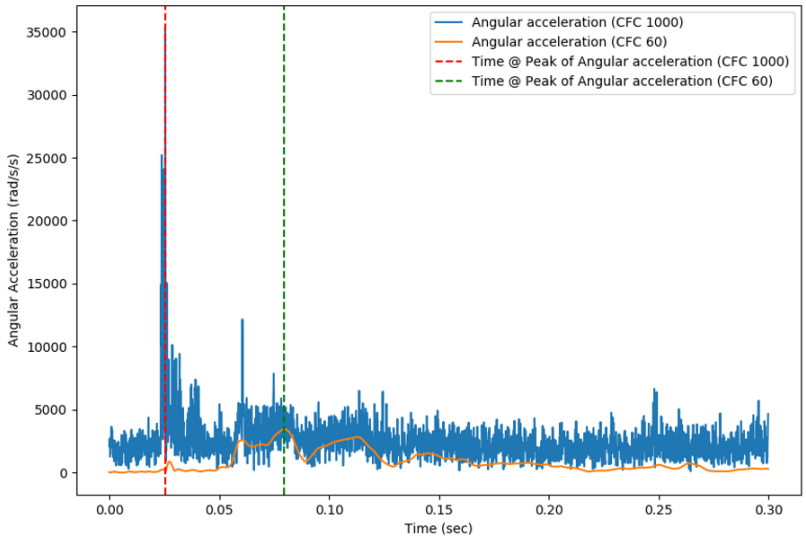

Fig. A14. Comparison of angular acceleration at CFC 1000 and at CFC 60: angular acceleration at CFC 60 computed from angular velocity at CFC 60

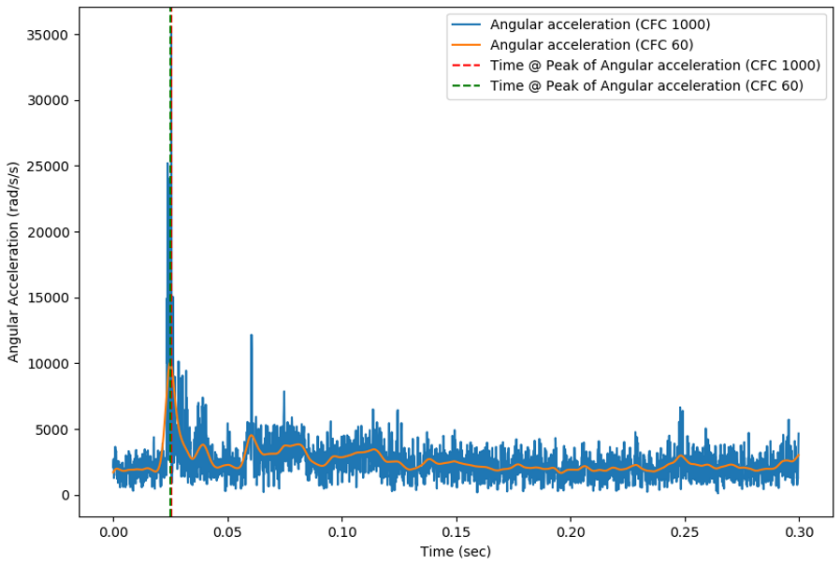

Fig. A15. Comparison of angular acceleration at CFC 1000 and at CFC 60: angular acceleration at CFC 60 computed from angular acceleration at CFC 1000

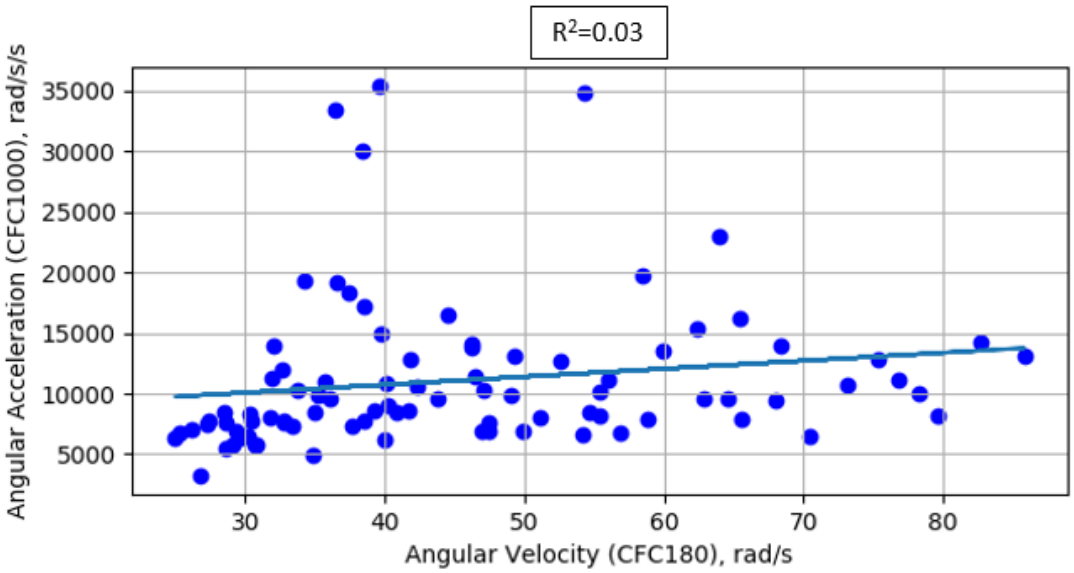

Fig. A16. Correlation plot between peak angular accelerations (CFC 1000) and peak angular velocities (CFC 180) for ARS data.

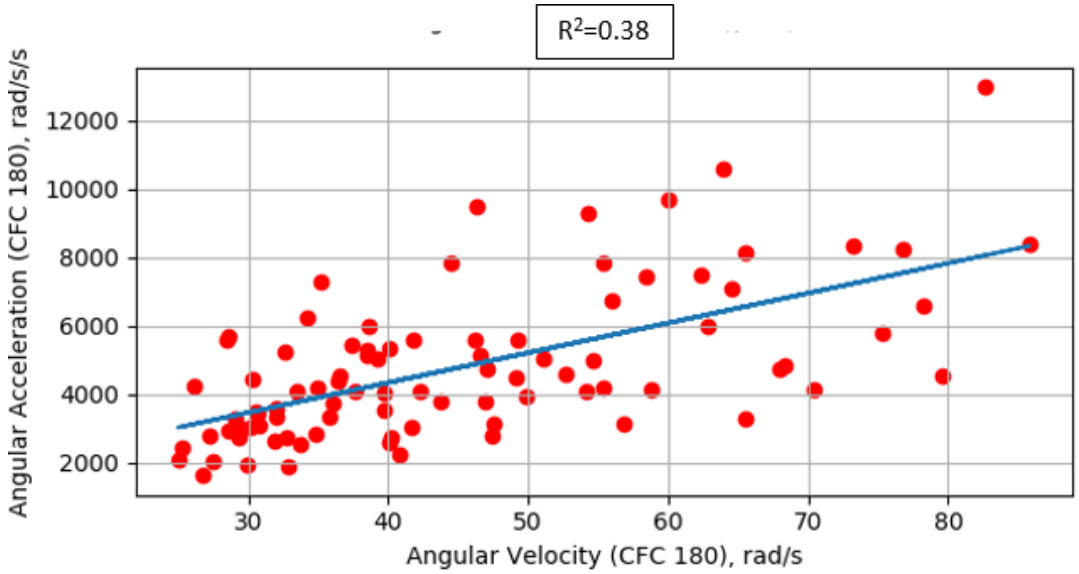

Fig. A17. Correlation plot between peak angular accelerations (CFC 180) and peak angular velocities (CFC 180) for ARS data.